Journal of the Physical Society of Japan
Vol. 68, No. 7, July, 1999, pp. 2186-2189

Strong Non-Ohmicity in Vertical Transport in Multilayered Quantum Hall Systems

Minoru KAWAMURA, Akira ENDO, Shingo KATSUMOTO* and Yasuhiro IYE*

Institute for Solid State Physics, University of Tokyo,
7-22-1 Roppongi, Tokyo 106-8666

(Received April 16, 1999)

Vertical transport in GaAs/AlGaAs superlattices has been studied in the quantum Hall regime. Both the in-plane and out-of-plane resistances exhibit an Arrhenius-type temperature dependence with small values of activation energy. At very low temperatures, the out-of-plane conductance becomes almost temperature independent and its values scale with the sample perimeter, indicating that the current is carried by the chiral surface states. The vertical transport in this regime exhibits distinct non-Ohmicity, suggesting the onset of bulk transport at high bias voltages. Rather strong non-Ohmicity is also observed in the low bias voltage region where the chiral surface state is responsible for the vertical transport.

KEYWORDS: vertical transport, GaAs/AlGaAs, semiconductor superlattice, quantum Hall effect, chiral surface state

A two-dimensional electron gas (2DEG) exhibits the quantum Hall effect (QHE) when it is placed in a strong perpendicular magnetic field. As two-dimensionality is an essential prerequisite for the occurrence of QHE, it is interesting to ask what happens when a degree of freedom for the motion perpendicular to the two-dimensional (2D) plane is introduced. This issue has been addressed both theoretically and experimentally since the early 1980s.[1-5] Störmer *et al.*[4] first demonstrated that quantized Hall conductance and vanishing diagonal resistivity can be observed in semiconductor superlattices. In semiconductor superlattices, the interlayer transfer integral t depends on such parameters as the barrier height, the barrier width and the well width. When the magnetic field is sufficiently strong that the cyclotron energy $\hbar\omega_c$ is larger than t, the density of states consists of a series of Landau subbands with the bandwidth $4t$. These subbands are further broadened by disorder. Each Landau subband consists of a central band of three-dimensionally extended states with localized tails on each side. When the in-plane transport exhibits the QHE, the Fermi energy is located in one of these localized tails.

The QHE in semiconductor superlattices has recently attracted renewed interest triggered by the theoretical prediction of the chiral surface state.[6] In an isolated 2DEG in the quantum Hall state, all the bulk states at the Fermi level are localized so that current (Hall current) is carried by the edge channels. These edge channels are free from backscattering because of their chirality. For the integer quantum Hall states, the edge states are described in terms of chiral Fermi liquid. When the interlayer transfer is introduced, the edge states in different layers are coupled to form a conducting surface state. Because of the chiral nature of the electronic motion in the edge state, localization (interference) effects are suppressed. Thus, despite their 2D character, the chiral surface states are expected to remain "metallic" at low temperatures, even if their conductivity is considerably less than e^2/h.[6] A recent experimental study by Druist *et al.*[7] shows the existence of such metallic states with a sheet conductivity σ_{zz} much less than e^2/h. In this letter, we report our experimental finding of prominent non-Ohmicity in the vertical transport in multilayered quantum Hall systems.

$GaAs/Al_{0.15}Ga_{0.85}As$ semiconductor superlattice wafers were grown by molecular beam epitaxy. They were grown in pairs of identical superlattices. One wafer for the vertical transport measurements was grown on an n^+GaAs(100) substrate and capped with a heavily doped layer. A second wafer for the lateral transport measurements was grown on a semi-insulating GaAs(100) substrate. The superlattice part consisted of 100 units of a 10-nm-wide GaAs well layer and a 15-nm-wide AlGaAs barrier layer. Only the central 5 nm of each AlGaAs layer was doped with Si donors to a concentration of 8.0×10^{23} m^{-3}. The relatively low Al content was chosen for the barrier layer to achieve a sufficiently large interlayer transfer integral t along the growth direction. The growth of the superlattice was performed at a relatively low substrate temperature, about 540°C, in order to prevent diffusion of the Si donors.

Figure 1(a) shows the calculated miniband structure along the growth direction (z-direction) using the Kronig-Penny model. Non-parabolicity of the conduction band and the slight difference in effective mass between GaAs and AlGaAs are neglected. A band-bending effect caused by the charge transfer from the barrier layer to the well layer is also neglected. The calculated band width along the z-direction is $4t = 0.12$ meV.

For the vertical transport measurements, square, columnar mesas were fabricated by photolithography and wet etching. Four mesas with different cross-sections of

* Also at *CREST, Japan Science and Technology Corporation.*

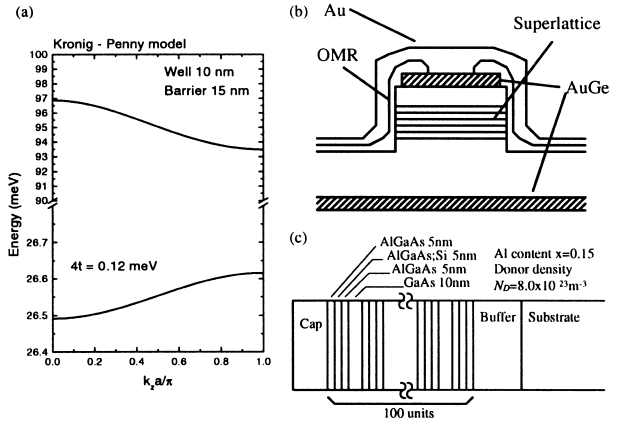

Fig. 1. (a) The dispersion relation along the z-direction. (b) Schematic picture of the sample for vertical tranport measurement. (c) Superlattice structure used in the present study.

50×50 μm^2, 100×100 μm^2, 200×200 μm^2 and 400×400 μm^2 were fabricated on a single chip. Electrical contact was achieved by a standard AuGe alloying technique with precautions to prevent Ge diffusion into the superlattice part. The overall sample geometry is shown in Fig. 1(b). The samples for the lateral transport measurements were patterned in a Hall bar shape. Magnetotransport measurements were carried out using a dilution refrigerator at temperatures down to 30 mK, in magnetic fields up to 15 T, using a superconducting solenoid. A standard ac lock-in technique was employed for the resistance measurements.

Figure 2(a) shows the magnetic-field dependence of the in-plane resistance R_{xx} and the Hall resistance R_{xy}. From the data, the sheet carrier density per layer and the Hall mobility are determined as $n_{2D} = 2.3 \times 10^{11}$cm^{-2}/layer and $\mu_{2D} = 6300$ cm^2/Vsec. The QHE is observed at filling factors $\nu = 2$ and $\nu = 1$. Note that the quantized Hall resistance is 1/100 of the usual value because we have a hundred 2DEGs in parallel. In Fig. 2(b), the magnetic-field dependence of the out-of-plane resistance R_{zz} is plotted for three mesas of different sizes. The sample sizes are 50×50 μm^2, 100×100 μm^2 and 200×200 μm^2. In the magnetic fields where the lateral transport exhibits the QHE, the out-of-plane resistance R_{zz} becomes maximum. In the inset of Fig. 2(b), the size dependence of the out-of-plane conductance $G_{zz} = 1/R_{zz}$ at $\nu = 2$ is plotted. G_{zz} is proportional to the mesa perimeter C, suggesting that the vertical transport at $\nu = 2$ is dominated by the surface states at this low temperature, as reported by Druist *et al.*[7)]

The temperature dependence of the out-of-plane conductance at $\nu = 2$ is shown in Fig. 3. Figure 3(a) (the upper panel) shows the 2D conductivity $\sigma_{zz}^{2D} = G_{zz}\frac{L}{C}$ scaled by the mesa perimeter, and Fig. 3(b) (the lower panel) shows the 3D conductivity $\sigma_{zz}^{3D} = G_{zz}\frac{L}{S}$ scaled by the mesa area S. Here, $L = 100 \times 25$ nm is the total thickness of the superlattice part. For these measurements, the excitation current was kept less than 3 nA. As the temperature is decreased, G_{zz} decreases rapidly following the Arrhenius-type temperature dependence, but it becomes nearly constant below 100 mK. As seen in Fig. 3(a), the constant values of the conductance below 100 mK are the same for the three samples when scaled

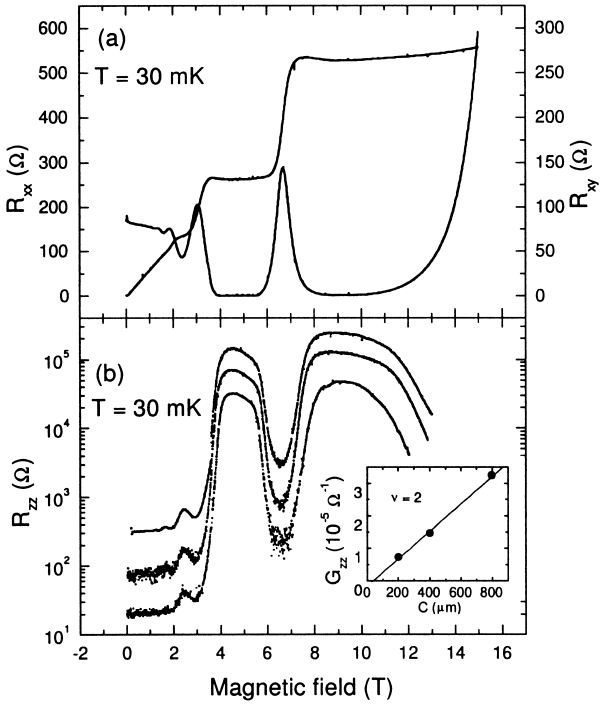

Fig. 2. (a) Magnetic field dependence of the in-plane resistance R_{xx} and the Hall resistance R_{xy}. (b) Magnetic field dependence of the out-of-plane resistance R_{zz}. The sample sizes are 50×50 μm^2, 100×100 μm^2 and 200×200 μm^2 from top to bottom. The inset shows the size dependence of the out-of-plane conductance G_{zz} at $\nu = 2$.

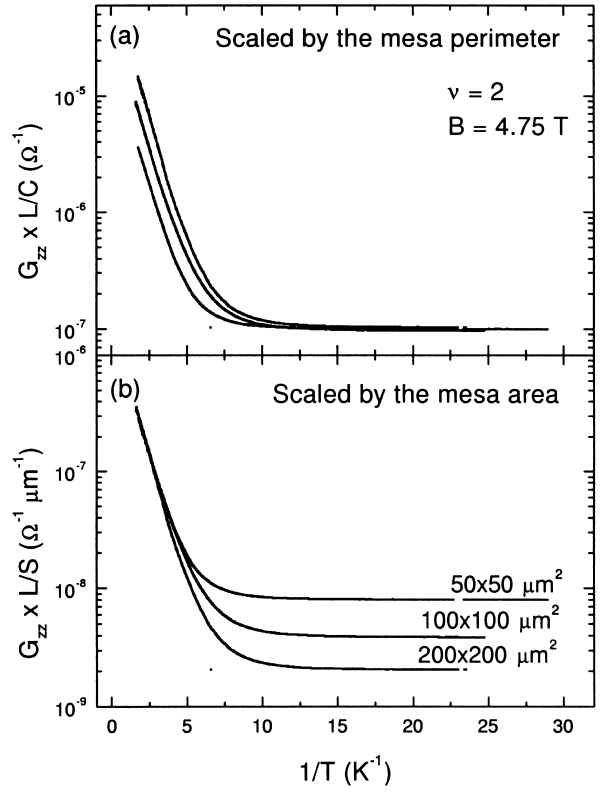

Fig. 3. Temperature dependence of G_{zz}. The vertical axis is scaled by (a) the mesa perimeter and by (b) the mesa area.

by the mesa perimeter. This indicates that there is a conducting sheath at the side face of the mesa, which remains "metallic" at low temperatures.[5-7] The measured temperature independent 2D sheet conductivity is $\sigma_{zz}^{\rm 2D}(\nu = 2) = 0.0027e^2/h$ which is much less than e^2/h. This value is about twice the value reported by Druist *et al.*[7] This difference may be understood in the following sense. According to the theory by Balents and Fisher,[6] the sheet conductivity at $\nu = N$ is given by

$$\sigma_{zz}^{\rm 2D}(\nu = N) = N\frac{e^2t^2\tau a}{2\pi\hbar^3 v}, \qquad (1)$$

where t is the interlayer transfer integral, τ is the scattering time, a is the interlayer spacing, and v is the electron velocity of the edge state. This equation contains two unknown parameters, τ and v, whose values are difficult to determine independently. In particular, the edge velocity v is sensitive to the detailed shape of the confinement potential, so it is difficult to estimate. This makes it difficult to compare the observed conductivity with the theoretical prediction. The difference between the results of Druist *et al.* and our results may also be attributed to the difference in these quantities.

As temperature is increased, the 2D conductivity curves scaled by the mesa perimeter start to deviate from each other. Above 100 mK, the conductance data for different mesa sizes are reduced to a single curve by scaling them by the mesa areas. This indicates that the dominant vertical transport at these high temperatures is through the bulk of the mesas. In the quantum Hall state for an isolated 2DEG, all the bulk states at the Fermi level are localized due to the presence of potential disorder. In the case of a multilayered quantum Hall system, if the spatial correlation between random potentials in different layers is small, the wave function cannot extend over many layers along the z-direction. The vertical transport through the bulk states can only occur at finite temperatures by thermal activation. The measured G_{zz} in the high-temperature region shows an Arrhenius-type temperature dependence,

$$G_{zz} \propto \exp(-E_{\rm a}/k_{\rm B}T), \qquad (2)$$

with the activation energy $E_{\rm a} = 0.95 \pm 0.05$ K which is much smaller than $\hbar\omega_{\rm c}/2 = 4.1$ meV $= 48$ K. The activation energy in the temperature dependence of the in-plane resistance R_{xx} measured on the same superlattice sample for the lateral transport is $E_{\rm a} = 1.0 \pm 0.1$ K, which is also much smaller than $\hbar\omega_{\rm c}/2$, in agreement with the earlier report by Störmer *et al.*[4] This is in contrast to the case of the conventional QHE in 2DEGs, where the activation energy which appears in the temperature dependence of R_{xx} is comparable to half the Landau level spacing $\hbar\omega_{\rm c}/2$.[8] It should be noted that although the Landau subband dispersion due to the interlayer transfer widens the central band of the extended states and changes the above quantity to $\frac{1}{2}\hbar\omega_{\rm c} - 2t$, the band width $4t = 0.12$ meV for the present sample is too small to account for the observed low values of the activation energy. Therefore, the relevant process is not the thermal excitation to the extended states at the center of the Landau subband, but the hopping among the localized states. The relevant activation energy for the latter process can be much smaller than $\frac{1}{2}\hbar\omega_{\rm c} - 2t$, although it is difficult to estimate since it is sensitive to the random potential profile.

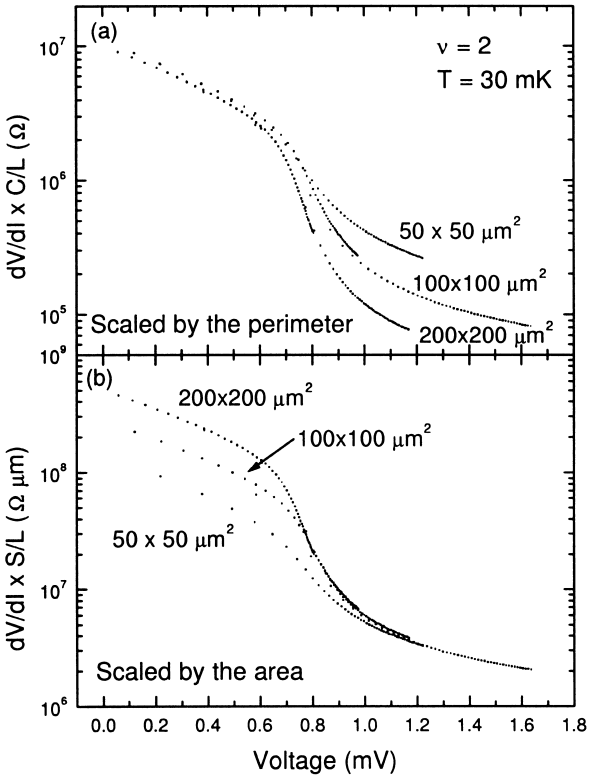

Fig. 4. Voltage dependence of the differential resistance $\mathrm{d}V/\mathrm{d}I$. The vertical axis is scaled by (a) the mesa perimeter and by (b) the mesa area.

Next, we turn our attention to the non-Ohmicity in the vertical transport in the quantum Hall states, and focus on the filling factor $\nu = 2$. The behavior at $\nu = 1$ is qualitatively similar. The experiments were carried out by measuring the differential resistance $\mathrm{d}V/\mathrm{d}I$ as a function of the dc bias current. In Fig. 4, the differential resistance $\mathrm{d}V/\mathrm{d}I$ is plotted against the voltage calculated from the data. Data for three samples with different cross-sections are shown. The temperature was kept at 30 mK during the measurements. As in Fig. 3, the vertical axis is scaled by the mesa perimeter in the upper panel (Fig. 4(a)) and by the mesa area in the lower panel (Fig. 4(b)). At voltages below ~ 0.5 mV, the differential resistivity scaled by the mesa perimeter collapses onto a single curve as seen in Fig. 4(a). On the other hand, the differential resistivity reduced by the mesa area is on a single curve at voltages above ~ 0.7 mV as shown in Fig. 4(b). Such scaling indicates that the current is carried mainly by the surface states in the low-voltage region but is extended to the bulk of the sample in the high-voltage region. The crossover from surface transport to bulk transport occurs in a fairly narrow range of the bias voltage. It is also noted that the differential resistance exhibits significant voltage dependence even in the region distant from the crossover.

Let us first consider the high-voltage region where the current flows mainly through the bulk of the sample.

The conduction occurs via hopping between the localized states near the Fermi level. Because the Fermi level is located in the tail part of the Landau subband, the relevant wave functions are highly localized. The localization length in the z-direction ξ_z is presumably not much greater than the interlayer distance. The thermally activated hopping current in the presence of a voltage bias is given by

$$I \propto \exp\left(-\frac{E_{\rm a}}{k_{\rm B}T}\right)\sinh\left(\frac{eV\xi_z/L}{k_{\rm B}T}\right) \sim \exp\left(-\frac{E_{\rm a}-eV\xi_z/L}{k_{\rm B}T}\right), \quad (3)$$

for $k_{\rm B}T \ll eV\frac{\xi_z}{L} \ll E_{\rm a}$. When $eV\frac{\xi_z}{L}$ approaches $E_{\rm a}$, the above formula is no longer applicable, and the voltage dependence will be less steep than the exponential form. The bias-voltage dependence of the differential resistance shown in Fig. 4(b) qualitatively agrees with the figure above.

We now consider the behavior in the low-voltage region, where the chiral surface sheath is responsible for the vertical transport. As noted earlier, the non-Ohmicity is also observed in the low-voltage region. We emphasize that this non-Ohmicity is quite substantial (the ordinate of Fig. 4 is in a log-scale), and it persists down to the lowest voltage of the present experiment. It is noteworthy that the sheet conductance in this region does not exhibit appreciable temperature dependence. This non-Ohmicity, together with the sheet conductance much less than e^2/h, reflects the marginally metallic nature of the chiral surface state. Provided that the phase coherence length l_ϕ is larger than the mesa perimeter C, increasing the ratio L/C will lead to a crossover from metallic behavior to 1D localized behavior.[9-11] The observed non-Ohmicity may be a type of precursor of this crossover. We hope that the present work will stimulate theoretical efforts to incorporate the effect of finite bias voltage in the description of the chiral surface state.

To summarize, we have observed distinct non-Ohmicity in the vertical transport in the multilayered quantum Hall system. The crossover from surface transport to bulk transport as a function of the bias voltage is fairly sharp. Non-Ohmic behavior in the high-voltage region can be interpreted in terms of the reduction of the effective activation energy. On the other hand, we can find no simple explanations for the non-Ohmicity in the low-bias-voltage region. The non-Ohmicity could be a clue to the elucidation of the marginally metallic character of the chiral surface state.

We thank T. Ohtsuki for valuable discussion on the localization effect in quantum Hall systems.

1) M. Ya. Azbel: Phys. Rev. B **26** (1982) 3430.
2) B. I. Halperin: Jpn. J. Appl. Phys. Suppl. **26** (1987) 1913.
3) T. Ohtsuki, B. Kramer and Y. Ono: J. Phys. Soc. Jpn. **62** (1993) 224.
4) H. L. Störmer, J. P. Eisenstein, A. C. Gossard, W. Wiegmann and K. Baldwin: Phys. Rev. Lett. **56** (1985) 85.
5) J. T. Chalker and A. Dohmen: Phys. Rev. Lett. **75** (1995) 4496.
6) L. Balents and M. P. A. Fisher: Phys. Rev. Lett. **76** (1996) 2782.
7) D. P. Druist, P. J. Turley, K. D. Maranowski, E. G. Gwinn and A. C. Gossard: Phys. Rev. Lett. **80** (1998) 365.
8) D. Weiss, E. Stahl, G. Weimann, K. Ploog and K. von Klitzing: Surf. Sci. **170** (1986) 285.
9) I. A. Grunzberg, N. Read and S. Sachdev: Phys. Rev. B **56** (1997) 13218.
10) S. Cho, L. Balents and M. P. A. Fisher: Phys. Rev. B **56** (1997) 15814.
11) V. Plerou and Z. Wang: Phys. Rev. B **58** (1998) 1967.